



**HAL**  
open science

## Properties of an amorphous magnesium silicate synthesized by precipitation

Marie Dietemann, Fabien Baillon, Fabienne Espitalier, Rachel Calvet,  
Philippe Accart, L-Mike Greenhill Hooper

### ► To cite this version:

Marie Dietemann, Fabien Baillon, Fabienne Espitalier, Rachel Calvet, Philippe Accart, et al.. Properties of an amorphous magnesium silicate synthesized by precipitation. ISIC 18 -18th International Symposium on Industrial Crystallization, Sep 2011, Zurich, Switzerland. p.112-113. hal-01753253

**HAL Id: hal-01753253**

**<https://hal.science/hal-01753253>**

Submitted on 7 Nov 2018

**HAL** is a multi-disciplinary open access archive for the deposit and dissemination of scientific research documents, whether they are published or not. The documents may come from teaching and research institutions in France or abroad, or from public or private research centers.

L'archive ouverte pluridisciplinaire **HAL**, est destinée au dépôt et à la diffusion de documents scientifiques de niveau recherche, publiés ou non, émanant des établissements d'enseignement et de recherche français ou étrangers, des laboratoires publics ou privés.

# Properties of an amorphous magnesium silicate synthesized by precipitation.

Marie Dietemann<sup>a,\*</sup>, Fabien Baillon<sup>a</sup>, Fabienne Espitalier<sup>a</sup>, Rachel Calvet<sup>a</sup>,  
Philippe Accart<sup>a</sup>, Mike Greenhill-Hooper<sup>b</sup>

<sup>a</sup>*Université de Toulouse, École des Mines d'Albi, FRE CNRS 3213, Centre RAPSODEE, Campus Jarlard F-81013 Albi Cedex 09, France*

<sup>b</sup>*Rio Tinto Minerals, 2 Place E. Bouillères, 31036 Toulouse, France*

---

## Abstract

Natural talc is a very interesting filler for plastic and rubber materials and paints because it improves their properties by delivering mechanical reinforcement and barrier effects. A good dispersion in a polymer matrix involves fine particles, with a size in the order of nanometer. But at the moment the main drawback of the use of natural talc is that, with conventional milling process, particles size under one micrometer are difficult and expensive to obtain. This study objective is to develop a process of magnesium silicate synthesis made by precipitation. This step is the first in the manufacturing process of synthetic talc. The resultant product will have properties that are not possible to obtain with the milling process, in particular particle size smaller than one micrometer.

The influence of different process parameters (reactants' addition mode, reactants' concentrations, synthesis temperature and ultrasound) on product properties is studied. Synthesized product is very agglomerated whatever process parameters but some parameters would enable to decrease agglomerates size. Reactants' addition by a mixing system with ultrasound during the synthesis would be the best in order to synthesize smallest particles. Moreover synthesis temperature and initial reactants' concentrations influence the nucleation rate and so agglomeration phenomenon.

*Keywords:* agglomeration, crystallisation, particle, powders, precipitation

---

---

\*Corresponding author

*Email addresses:* Marie.Dietemann@mines-albi.fr (Marie Dietemann),

## 1. Introduction

Natural talc is an interesting material that can be used as high performance filler in polymers. It improves their properties, for instance, excellent mechanical reinforcement and barrier effects are improved (Ciesielczyk, Krysztafkiewicz, Bula and Jesionowski, 2010). In plastics, talc improves tensile and transverse strength and modulus of elasticity (Tufar, 2000). In rubbers, talc is interesting because of its lubricating properties (Tufar, 2000). Talc also improves resistance to corrosion of paints. It also changes their flow properties, makes sprawl easier and reinforces hiding power (Martin, 1999). However, an homogeneous dispersion is necessary to obtain these different performances. A good dispersion in a polymer matrix needs, in an ideal case, nano-sized particles (Martin, Ferret, Lèbre, Petit, Grauby, Bonino, Arseguel and Decarreau, 2006). However, it is difficult to obtain particles smaller than one micrometer using conventional milling processes. An alternative method to milling is the chemical synthesis of talc. Two steps are necessary. The first step consists of silicate magnesium precipitation with the production of an amorphous solid. An second step is necessary to convert the amorphous solid into a crystalline lamellar nano-sized particles with a talc-like structure. Amorphous or crystalline magnesium silicate particles can be used as filler particles.

The second step of the process of synthetic talc has been the subject of several investigations by Lèbre (2007). But, except works of Ciesielczyk, Krysztafkiewicz and Jesionowski (2005, 2007), Ciesielczyk et al. (2010), few investigations have been held about the precipitation. [The aim of this work is to study the influence of precipitation parameters on product properties.](#)

Though some process parameters, such as reactants' concentrations, temperature or use of a premixing system or ultrasound present an influence on properties of a precipitated product, in particular on particles size distributions (Mersmann, 1999). According to Dodds, Espitalier, Louisnard, Grossier, David, Hassoun, Baillon, Gatumel and Lyczko (2007), ultrasound used during the synthesis also influence particle size. It has been shown that  $\text{BaSO}_4$ ,  $\text{K}_2\text{SO}_4$ ,  $\text{TiO}_2$  and sucrose crystals are smaller when crystallisation or precipitation is made with ultrasound. In this work, ultrasound influence on particles size distributions is studied.

Synthesized particles size distributions and agglomeration phenomenon is the most important property observed in this study.

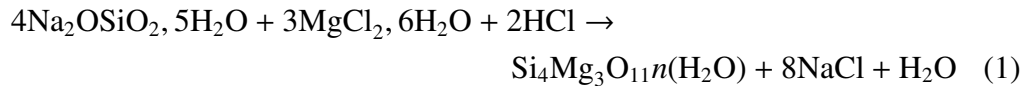
---

Fabienne.Espitalier@mines-albi.fr (Fabienne Espitalier),  
Mike.GreenhillHooper@borax.com (Mike Greenhill-Hooper)

## 35 2. Experimental

### 36 2.1. Materials

37 The amorphous magnesium silicate is synthesized by a precipitation between  
38 a sodium metasilicate solution ( $\text{Na}_2\text{OSiO}_2$ ) and an acid magnesium chloride solu-  
39 tion ( $\text{MgCl}_2$ ), according to the following equation 1 (Martin et al., 2006):



40 Reactants are aqueous solutions of sodium metasilicate (purity 100%), called re-  
41 actant 1, and of magnesium chloride (purity 97%), called reactant 2 (supplier Pro-  
42 labo). Molar ratio Mg/Si is always 0.75, corresponding to that of natural talc.  
43 In order to maintain stoichiometry of reaction, hydrochloric acid 1M is added in  
44 aqueous solution of magnesium chloride (supplier Prolabo). Demineralised water  
45 is used. At the end of the synthesis, a part of the solid is dried at  $550^\circ\text{C}$  during  
46 5 hours. The solid weight loss permits to estimate the value of  $n$ . It's ranged  
47 between 4.6 and 4.85. The influence of reactants' addition mode, reactants' con-  
48 centrations ( $C_{\text{MgCl}_2,6\text{H}_2\text{O}} = 0.81, 1.49$  and  $1.88 \text{ mol.L}^{-1}$ ;  $C_{\text{Na}_2\text{SiO}_3,5\text{H}_2\text{O}} = 0.71, 1.43$   
49 and  $1.97 \text{ mol.L}^{-1}$ ), temperature (20, 40 and  $50^\circ\text{C}$ ) and ultrasound in the Y-mixing  
50 system on product properties is studied.

### 51 2.2. Procedures and Methods

#### 52 2.2.1. Synthesis of magnesium silicate

53 This synthesis is made in a 1L vessel with four baffles, at constant temperature  
54 and stirrer rate of 600 rpm. The mixing device is an PTFE helix propeller with four  
55 squared blades. Its diameter is about 4 cm. Three addition modes have been tested.  
56 The first mode is the slow addition, drop by drop, of one reactant into the other  
57 (Fig. 1a). The second mode is the fast addition of one reactant into the other. This  
58 mode is not depicted in Fig. 1 because materials are the same as slow addition.  
59 The only difference is that magnesium chloride solution is added instantaneously  
60 instead of drop by drop. In the third mode, reactants are mixed in a Y-mixing  
61 system ( $H \approx 6 \text{ cm}$ ,  $D \approx 4 \text{ cm}$ ,  $V \approx 42 \text{ mL}$ )(Fig. 1b). Peristaltic pumps are used  
62 in order to feed solutions into the mixing system. Rates and speeds of flow are  
63 respectively  $125.25 \text{ g.min}^{-1}$  and  $0.30 \text{ m.s}^{-1}$  for sodium metasilicate solution and  
64  $81.30 \text{ g.min}^{-1}$  and  $0.19 \text{ m.s}^{-1}$  for magnesium chloride solution. Mixing occurs  
65 inside the mixing system at the exit of pipes which come from pumps. At the exit

66 of the mixing system, the suspension is poured in the vessel which is initially filled  
67 with 100 mL of demineralised water. Ultrasound can be used in the Y-mixing  
68 system (f=20 kHz).

69 In the Y-mixing system, the Reynolds number  $Re_Y$  is given by the following  
70 equation (Eq. 2):

$$Re_Y = \frac{\rho Lu}{\mu} = 1\ 184 \quad (2)$$

71 with  $\rho$ , the density of the suspension ( $\text{kg.m}^{-3}$ ),  $L$ , the Y-mixing system diameter  
72 (m),  $u$ , the flow speed ( $\text{m.s}^{-1}$ ) and  $\mu$ , the viscosity of the suspension ( $\text{kg.m}^{-1}.\text{s}^{-1}$ ).

This value of the Reynolds number indicates an intermediate range between laminar and turbulent flows. In the vessel, the Reynolds number of mixing  $Re_v$  is given by the following equation (Eq. 3):

$$Re_v = \frac{\rho ND^2}{\mu} = 21\ 876 \quad (3)$$

73 with  $\rho$ , the density of the suspension ( $\text{kg.m}^{-3}$ ),  $N$ , the revolution speed of the  
74 mixing device ( $\text{r.s}^{-1}$ ),  $D$ , the mixing device diameter (m) and  $\mu$ , the viscosity of  
75 the suspension ( $\text{kg.m}^{-1}.\text{s}^{-1}$ ).

76 This value indicates a turbulent range. The Reynolds number in the vessel  
77 enables to determine the power number  $N_p$  for the used mixing device ( $N_p$  is 1 in  
78 this study) and then the energy dissipation  $\epsilon$  (Eq. 4):

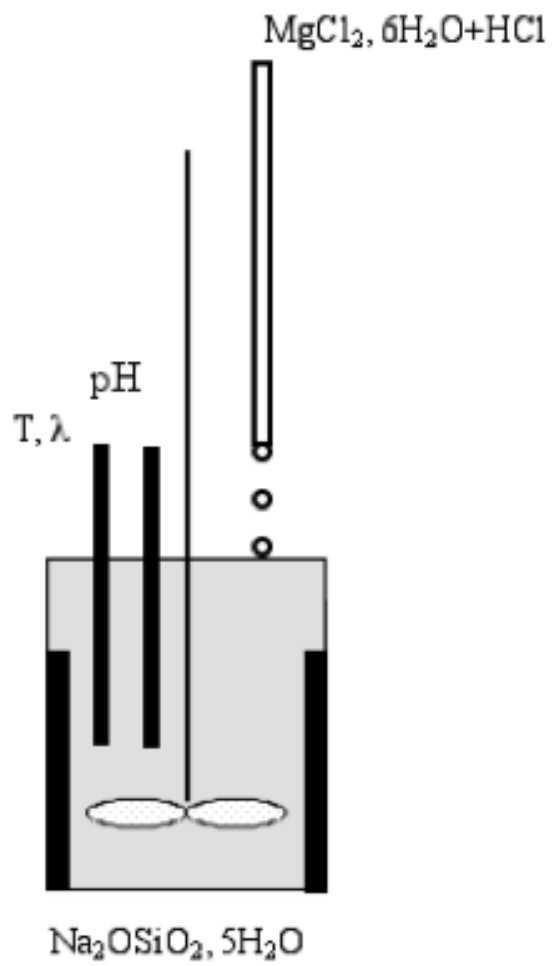
$$\epsilon = \frac{N_p N^3 D^5}{V} = 0.18 \text{ W.kg}^{-1} \quad (4)$$

79 with  $V$ , the vessel volume ( $\text{m}^3$ ).

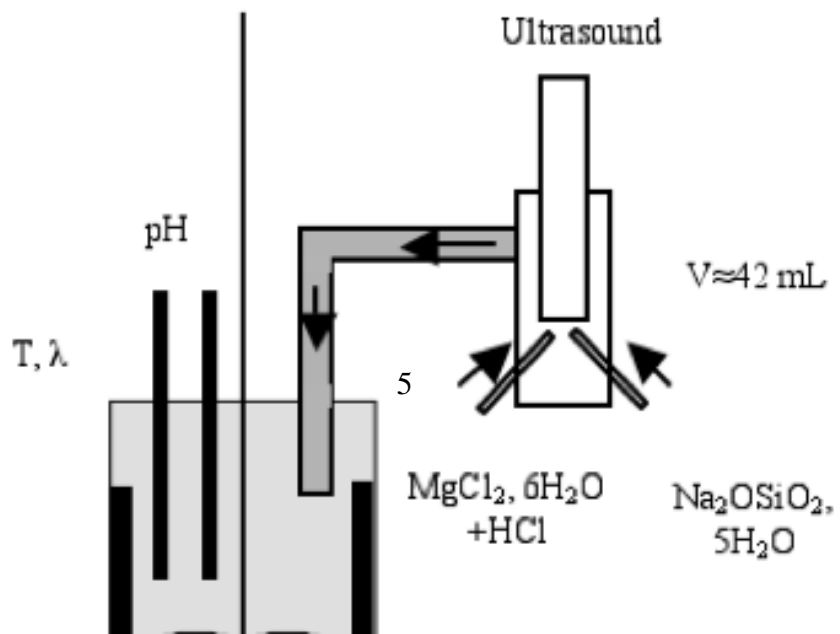
80 When trials are made at a higher temperature than the room temperature (40  
81 or 50°C) reactants are heated with hotplates. The vessel is heated at 40 or 50°C  
82 thanks to a constant-temperature bath.

83 During the synthesis, the conductivity and the temperature of the solution are  
84 measured. Getting the stability of the conductivity enables to determine the end  
85 of the reaction. The conductivity of a solution is influenced by the temperature.  
86 So conductivities measured at different temperatures must be corrected by a tem-  
87 perature coefficient in order to be compared. The temperature coefficient  $\theta$  ( $\%/^\circ\text{C}$ )  
88 is calculated by the following equation (Eq. 5):

$$\theta = \frac{(\lambda_{T_2} - \lambda_{T_1}) * 100}{(T_2 - T_1) * \lambda_{T_1}} \quad (5)$$



(a)



89 with  $\lambda_{T_2}$ , the conductivity measured at the temperature  $T_2$ ,  $\lambda_{T_1}$ , the conductivity  
90 measured at the temperature  $T_1$  which is close to the reference temperature (20  
91 °C). Conductivities unit is  $S.cm^{-1}$  and temperatures unit is °C.

92 In this work, the temperature coefficient  $\theta$  has been measured with a solution  
93 containing ... for a temperature range of 20-40 °C . A value of 2.1 %/°C has been  
94 obtained.

95 At the end of the synthesis, the suspension is filtered with a Büchner-membrane  
96 system. The cake is then washed four times with water, so salt formed during the  
97 synthesis is eliminated. The product is then dried at 100°C during 12 hours. At  
98 the end of the drying step, the product is very agglomerated that's why it's ground  
99 by a laboratory impact mill (coffee mill).

### 100 2.2.2. *Properties of synthetic magnesium silicate*

101 Suspension and synthesized powders are submitted for physical chemistry  
102 analysis.

103 Samples are taken of the suspension in order to be analysed by dynamic light  
104 scattering technique using Malvern Mastersizer 2000. This enables particle size  
105 distribution to be followed during the synthesis. Suspension is diluted with water  
106 in the granulometer. Ultrasound can be applied during the size measurement.  
107 Figure 2 shows the influence of ultrasound applied during the size analysis on  
108 particle size distribution. After ultrasound use, size distribution is shifted towards  
109 fine particles. It must be due to ultrasound which cause disaggregation of the  
110 solid. Over two minutes of ultrasound, particles size distribution doesn't change  
111 any more. So every sample is subjected to ultrasound during two minutes.

112 In order to define surface morphology and agglomeration state of particles,  
113 dried products are examined by scanning electron microscopy (SEM-FEG, Philips  
114 XL 30).

115 Density of dried products is measured using a Micrometrics AccuPyc 1330  
116 helium pycnometer.

117 BET surface area of dried products is estimated using a Micrometrics ASAP  
118 2010 K2 apparatus and getting nitrogen adsorption/desorption isotherms. Meso-  
119 porous volume is calculated by using the Barret, Joyner and Halenda method  
120 (B.J.H. method) on the desorption field of the adsorption/desorption isotherm.  
121 Micro-porous volume is calculated by using the Horvath-Kawazoe method (H.  
122 -K. method) with split pore geometry on the adsorption field of the adsorption/desorption  
123 isotherm.

124 Analysis by X-Ray diffraction are also made on dried products using the  
125 diffractometer X'Pert Philips Pan Analytical with  $CuK\alpha$  radiation source. Mea-

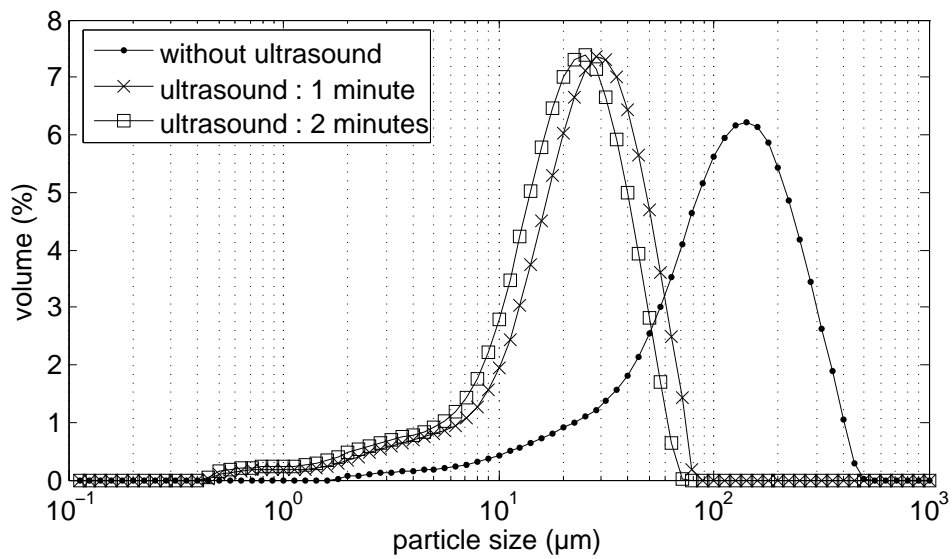


Figure 2: Influence of ultrasound applied during the size analysis on particle size distribution (addition mode: slow addition,  $C_{\text{MgCl}_2 \cdot 6\text{H}_2\text{O}} = 1.49 \text{ mol.L}^{-1}$ ,  $T=20^\circ\text{C}$ , samples taken of after 210 minutes).



126 surement and duration steps are respectively  $2\theta=0.0334^\circ$  and 50 seconds.

### 127 2.2.3. Amorphous magnesium silicate solubility

128 Some trials on magnesium silicate solubility are made at different tempera-  
129 tures. Solubility is measured in water for a constant concentration of NaCl equal  
130 to  $0.63 \text{ mol.L}^{-1}$ . ~~The concentration of NaCl is the same as concentration in the~~  
131 ~~vessel during the synthesis ( $0.63 \text{ mol.L}^{-1}$ ).~~ Dried and milled magnesium silicate  
132 is introduced in the aqueous solution kept at some six constant temperatures (20,  
133 30, 35, 40, 50 and  $60^\circ\text{C}$  plus ou moins ??). Conductivity is measured as a function  
134 of time, while suspension is agitated (Fig. 3).

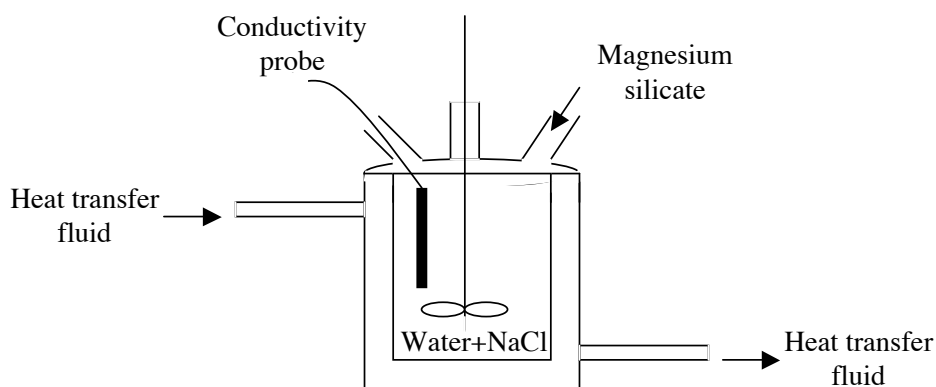


Figure 3: Experimental scheme of solubility trials.

## 135 3. Results and discussion

### 136 3.1. Amorphous magnesium silicate solubility

137 Figure 4 shows the evolution of suspension conductivity as function of time  
138 at constant temperature. After two hours, the conductivity attains a plateau. Sta-  
139 bility of conductivity reveals equilibrium state of the suspension. The value at  
140 the plateau increases with the temperature. So amorphous magnesium silicate  
141 solubility seems to increase when temperature increases (Fig. 4).

### 142 3.2. Evolution of the conductivity during synthesis

143 The conductivity of the suspension is measured in the vessel during the synthe-  
144 sis. The evolution of the conductivity is influenced by the addition mode (Fig. 5).

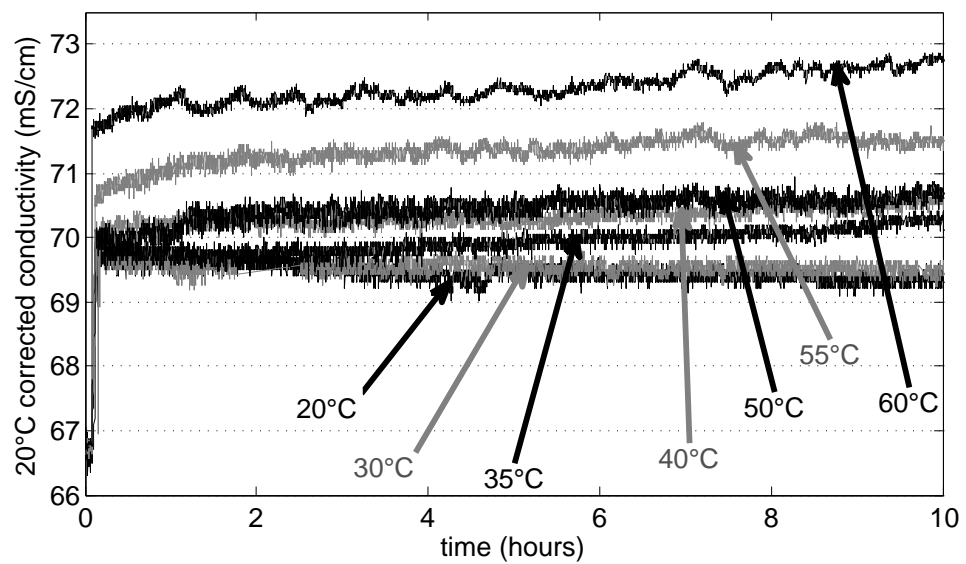


Figure 4: Evolution of conductivity as a function of time and temperature for a constant concentration of NaCl equal to  $0.63 \text{ mol.L}^{-1}$ .

145 In the process with the slow addition, the conductivity firstly slowly decreases  
146 because of the solid formation by addition of magnesium chloride solution in the  
147 vessel. The conductivity is then stable before increasing at the end of the addi-  
148 tion. This increase is not explained yet. In the process with the fast addition, the  
149 conductivity fastly decreases because of the solid formation by addition of mag-  
150 nesium chloride solution in the vessel. The conductivity is then stable. The final  
151 value is the same as in the process with the slow addition. In the process with the  
152 mixing system, the conductivity firstly fastly increases because the vessel is ini-  
153 tially filled with water. The conductivity is then stable because the solid is formed  
154 before being poured in the vessel. In this case, the final conductivity is lower than  
155 slow and fast addition. The desupersaturation seems to be more important in the  
156 case of reactant pre-mixing.

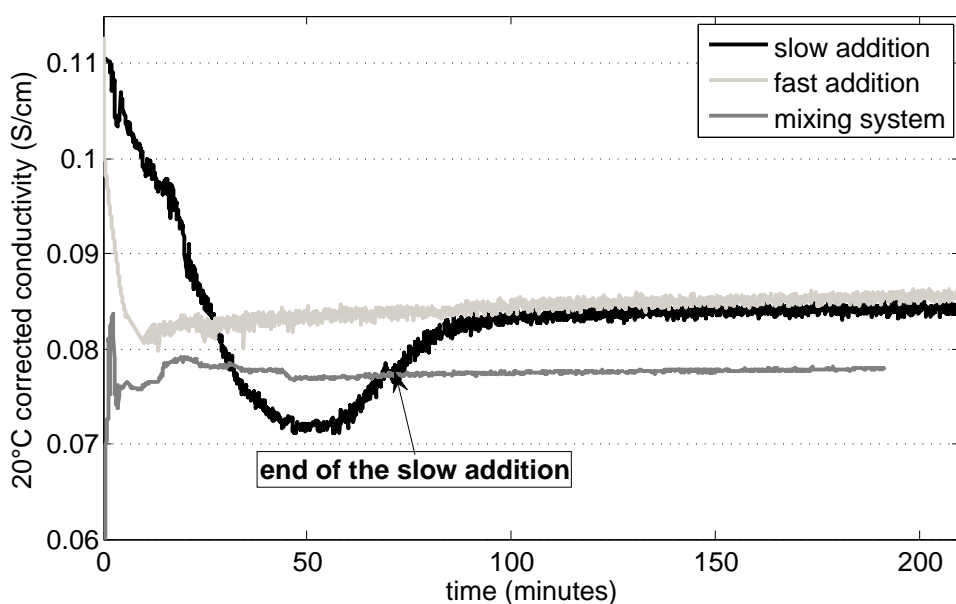


Figure 5: Evolution of the conductivity as a function of time and addition mode ( $C_{\text{MgCl}_2 \cdot 6\text{H}_2\text{O}} = 1.49 \text{ mol.L}^{-1}$ ,  $T=20^\circ\text{C}$ ).

157 The conductivity of the suspension at the end of the synthesis, is also influ-  
158 enced by the temperature and the NaCl concentration (Fig. 6). When NaCl con-  
159 centration is fixed constant, the final corrected conductivity increases with the  
160 temperature in agreement with the evolution of solubility as function of tempera-  
161 ture. When the temperature is fixed constant, the final conductivity increases with

162 the NaCl concentration. It's explained by the increase of dissolved ions when  
163 NaCl concentration increases. From these different results on synthesis and sol-  
164 ubility measurements, the solubility of amorphous magnesium silicate increases  
165 with temperature and NaCl concentration or ionic strength.

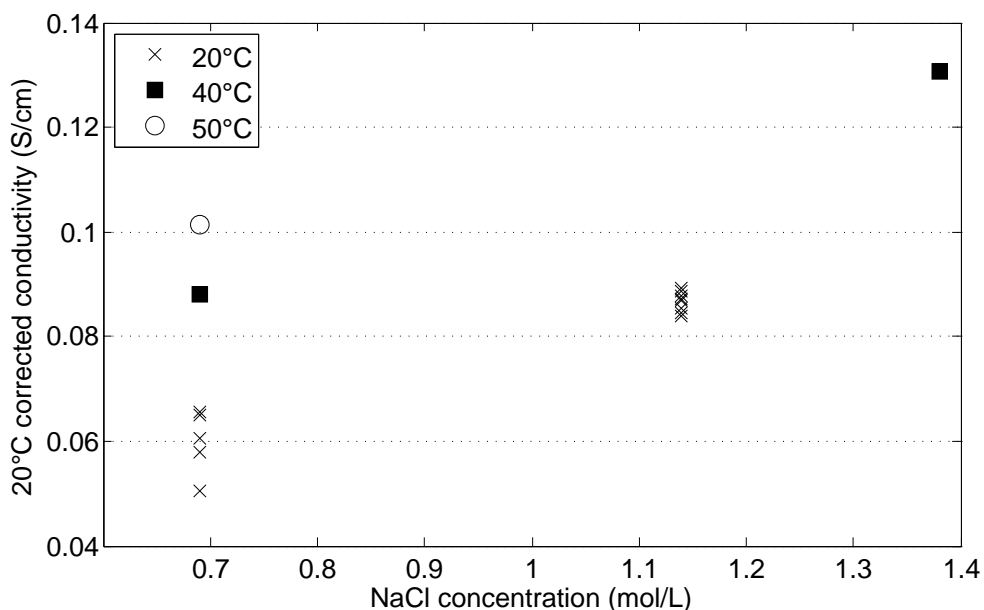


Figure 6: Conductivity at the end of synthesis as a function of temperature and NaCl concentration.

### 166 3.3. Properties of synthetic magnesium silicate

#### 167 3.3.1. Amorphous state of the powder

168 Diffractograms get by X-Ray diffraction analyses show that all synthesized  
169 magnesium silicate solids are amorphous. The diffractogram (Fig. 7) doesn't  
170 present any real peak, only a large initiation of a peak at  $2\theta=46.5^\circ$ . But it can't be  
171 exploited because of its low intensity.

172 Whatever studied process parameters, product ~~get after the step of~~ obtained  
173 by precipitation is always amorphous. These results are in compliance with works  
174 of Ciesielczyk et al. (2005, 2007). They have showed that precipitated magnesium  
175 silicate is amorphous and this form is independent of the precipitation temperature  
176 and addition mode.

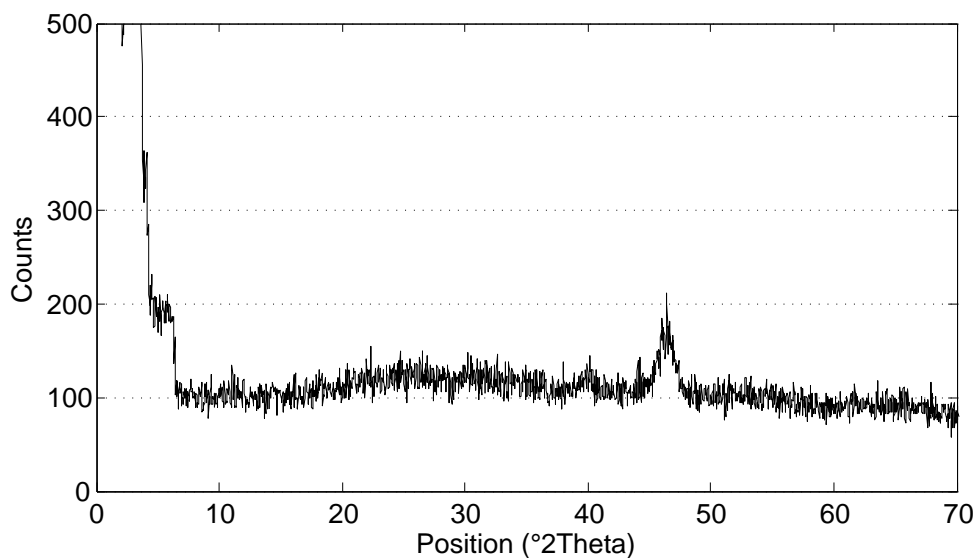


Figure 7: Diffractogram of a product (addition mode: parallel with mixing system,  $C_{\text{MgCl}_2 \cdot 6\text{H}_2\text{O}} = 0.81 \text{ mol.L}^{-1}$ ,  $T=20^\circ\text{C}$ ) get by X-Ray diffraction at  $0.154 \text{ nm}$  (Cu) (measurement step  $2\theta = 0.0334^\circ$ ; duration step = 50 seconds).

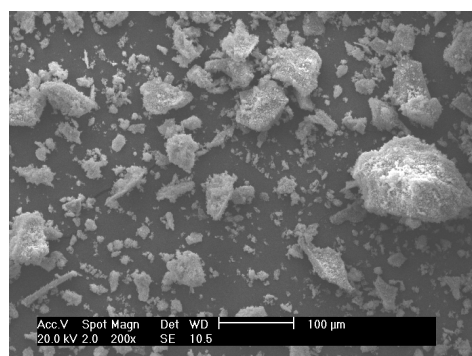
177 *3.3.2. Agglomeration state of the powder*

178 The dry solid is composed of fine particles strongly agglomerated (Fig. 8).  
 179 Amorphous product seems to be made up of two kinds of agglomerates. Sec-  
 180 ondary agglomerates (Fig. 8a and 8b) are made up of primary agglomerates (Fig. 8c)  
 181 which are made up of primary spherical particles (Fig. 8d). This kind of structure  
 182 is observed whatever process parameters.

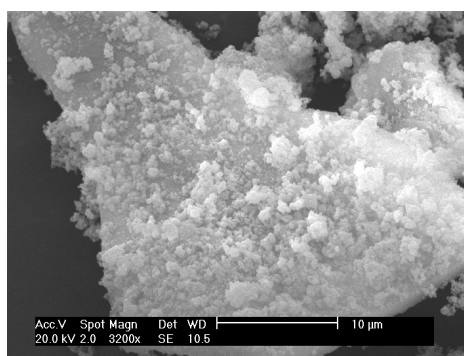
183 The Table 1 summarizes suspension and solid properties (corrected conductiv-  
 184 ity at the end of synthesis  $\lambda_s$ ,  $d_{50}$ ,  $d_{32}$ , density, specific surface area) as a function  
 185 of operating conditions.

186 The product density seems to be independent of studied operating conditions:  
 187  $2.195 \pm 0.036 \text{ g.cm}^{-1}$ .

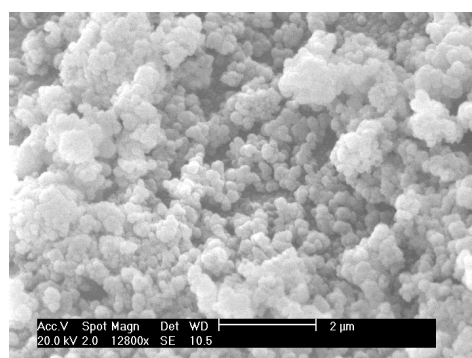
188 Except trial 1, the specific surface area varies conversely to the diameters  $d_{50}$   
 189 and  $d_{32}$ : when the diameter increases, the specific surface area decreases. The  
 190 result of the trial 1 is different but it's the only specific surface area measured with  
 191 the slow addition. This difference might be due to the addition mode. Maybe with  
 192 the slow addition the magnesium silicate structure is formed differently than with  
 193 the mixing system. More analysis would be necessary on products synthesized  
 194 with the slow addition in order to conclude.



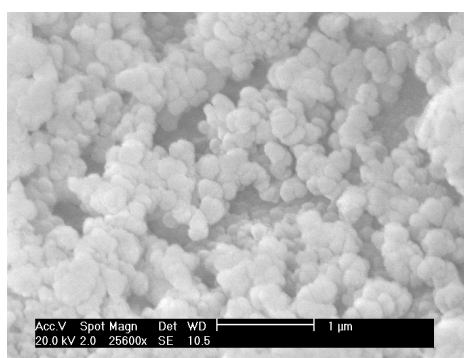
(a) x200



(b) x3200



(c) x12800



(d) x25600

Figure 8: SEM analysis of products synthesized by slow addition,  $C_{\text{MgCl}_2 \cdot 6\text{H}_2\text{O}} = 1.49 \text{ mol.L}^{-1}$ ,  $T=20^\circ\text{C}$ .

Trial	Addition mode	Temperature (°C)	[MgCl <sub>2</sub> , 6H <sub>2</sub> O] (mol.L <sup>-1</sup> )	[Na <sub>2</sub> SiO <sub>3</sub> , 5H <sub>2</sub> O] (mol.L <sup>-1</sup> )	$\lambda_f$ (mS.cm <sup>-1</sup> )	d <sub>50</sub> (μm)	d <sub>32</sub> (μm)	Density (g.cm <sup>-3</sup> )	Sp
1	slow	20	1.49	1.43	83.8	20.9	9.9	2.209	
2	fast	20	1.49	1.43	86.4	26.1	13.1	2.206	
3	mixing system +ultrasound	20	1.49	1.43	77.9	19.2	6.5	2.203	
4	mixing system (no ultrasound)	20	0.81	0.71	58.7	11.2	5.7	2.131	
5	mixing system +ultrasound	20	0.81	0.71	64.2	4.2	2.3	2.147	
6	mixing system +ultrasound	40	0.81	0.71	63,7	4.4	2.7	2.222	
7	mixing system +ultrasound	40	1.97	1.88	94.6	17.3	7.1	2.222	
8	mixing system +ultrasound	50	0.81	0.71	64.3	5.9	2.8	2.220	

Table 1: Physical properties of synthetic magnesium silicates.

195 Synthesized magnesium silicate has micro-pores: gas is absorbed at very low  
196 relative pressures (Fig. 9). The mean diameter of micro-pore is about 0.65 nm  
197 and the micro-porous volume is 0.10 m<sup>3</sup>.g<sup>-1</sup>. The product presents only an inter  
198 primary agglomerates meso-porosity. Meso-pores might be inside secondary  
199 agglomerates, between primary agglomerates whereas micro-pores might be in-  
200 side primary agglomerates, between primary particles. The meso-pore diameter  
201 is 23 nm and the meso-porous volume is 0.46 m<sup>3</sup>.g<sup>-1</sup>. The hysteresis observed is  
202 probably due to this inter-granular porosity.

### 203 3.4. Influence of reactants' addition mode

204 Particle size distributions (Fig. 10) show there is an influence of reactants'  
205 addition mode. The three particle size distributions have the same width (700  
206 nm-80 μm) but with the addition by mixing system, particle size distribution is  
207 composed of smaller particles under 7 μm. With the fast addition, particle size  
208 distribution shows less agglomerates under 10 μm but more agglomerates between  
209 10 and 100 μm. These differences may be due to the micromixing effect.

210 SEM analysis (Fig. 11) confirm these observations: product synthesized with  
211 the mixing system and ultrasound is made up of smaller particles.

### 212 3.5. Influence of ultrasound during the synthesis

213 At low concentrations ( $C_{\text{MgCl}_2,6\text{H}_2\text{O}} = 0.81 \text{ mol.L}^{-1}$ ), with ultrasound used dur-  
214 ing the synthesis made by parallel reactants' addition with the mixing system,

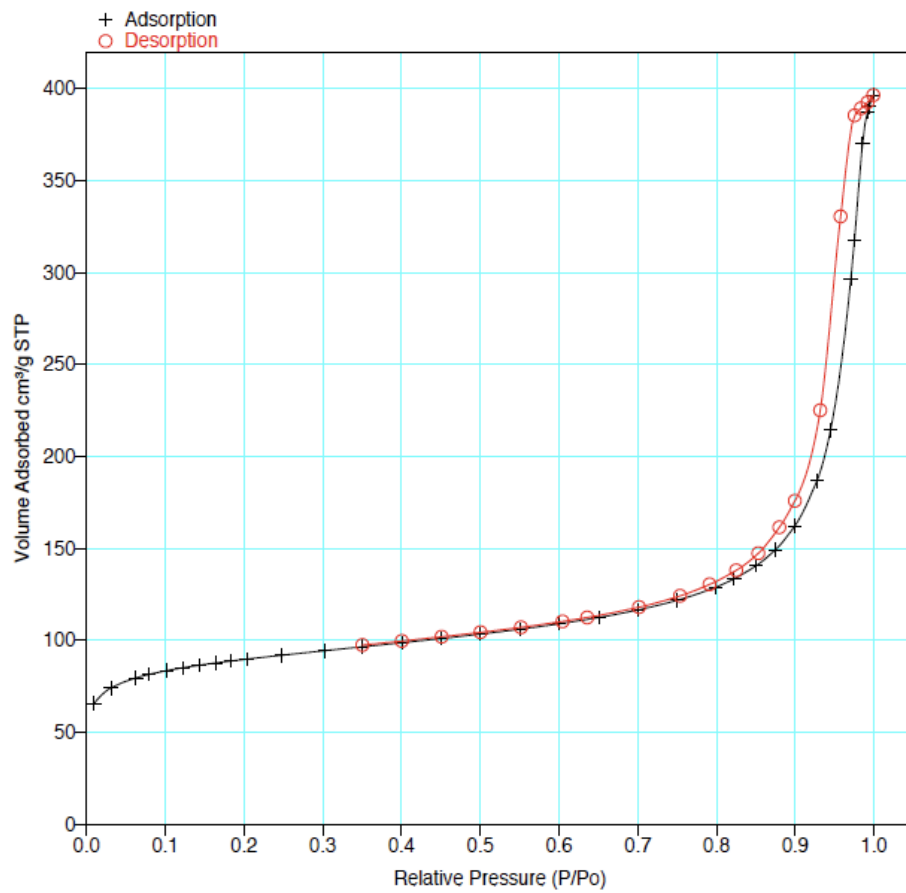


Figure 9: Adsorption/desorption isotherm of a magnesium silicate (parallel reactants' addition with mixing system and ultrasound are used,  $C_{MgCl_2 \cdot 6H_2O} = 0.81 \text{ mol.L}^{-1}$ ,  $T=20^\circ\text{C}$ ).



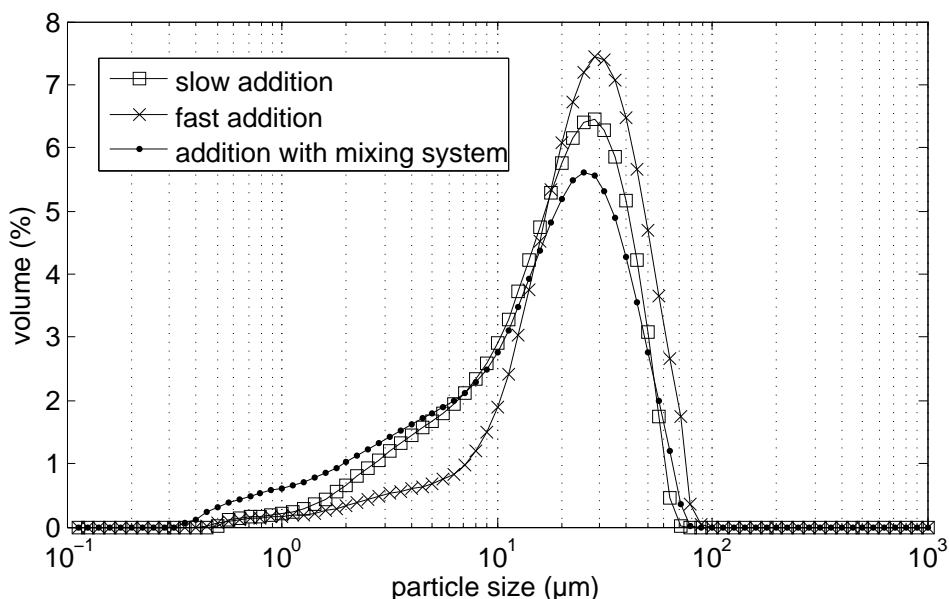


Figure 10: Particle size distributions as a function of addition modes ( $C_{\text{MgCl}_2 \cdot 6\text{H}_2\text{O}} = 1.49 \text{ mol.L}^{-1}$ ,  $T=20^\circ\text{C}$ , samples taken of after 90 minutes).

215 smaller particles are observed (Fig. 12). Particle size distributions are very dif-  
 216 ferent. Particle sizes are smaller than  $20 \mu\text{m}$  with ultrasound as against  $100 \mu\text{m}$   
 217 without ultrasound in the mixing system.

218 Ultrasound would reduce particles size, prevent agglomerates from forming  
 219 and would break flocs already formed during the mixing of reactants. Same re-  
 220 sults on size reduction have been found with the synthesis of  $\text{BaSO}_4$ ,  $\text{K}_2\text{SO}_4$ ,  
 221  $\text{TiO}_2$  and sucrose particles (Dodds et al., 2007). In these works, ultrasound treat-  
 222 ment produces a decrease of particle size in comparison with the same physical or  
 223 chemical process without ultrasound.

224 With ultrasound in the mixing system, the specific surface area of the product  
 225 is  $350 \text{ m}^2 \cdot \text{g}^{-1}$  as against  $257 \text{ m}^2 \cdot \text{g}^{-1}$  without ultrasound (Table 1).

### 226 3.6. Influence of reactants' concentrations

227 Particle size distribution is very influenced by initial reactants' concentrations.  
 228 At high concentrations, in the same other process conditions, distribution is clearly  
 229 shifted towards large sizes (Fig. 13).

230 At high concentrations ( $1.49 \text{ mol.L}^{-1}$ ), the particle size distribution is almost  
 231 the same as distribution obtained with no mixing system fast addition).

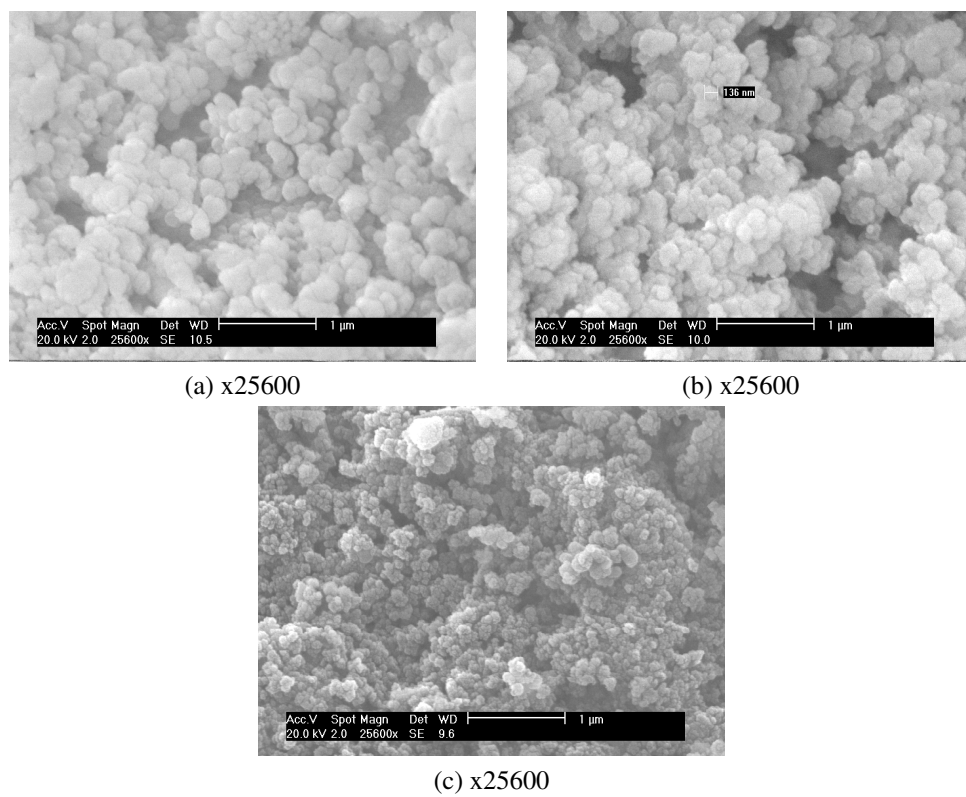


Figure 11: SEM analysis of products synthesized by slow addition (a), fast addition (b) and with the mixing system and ultrasound (c) ( $C_{\text{MgCl}_2 \cdot 6\text{H}_2\text{O}} = 1.49 \text{ mol.L}^{-1}$ ,  $T=20^\circ\text{C}$ ).

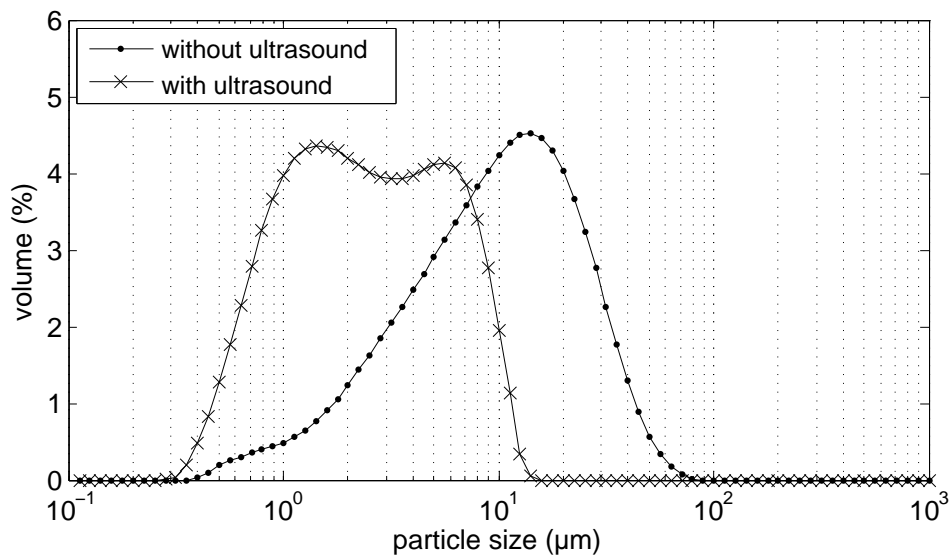


Figure 12: Particle size distributions as a function of ultrasound used during the synthesis. Parallel reactants' addition with mixing system is used ( $C_{\text{MgCl}_2 \cdot 6\text{H}_2\text{O}} = 0.81 \text{ mol.L}^{-1}$ ,  $T=20^\circ\text{C}$ , samples taken of after 90 minutes).

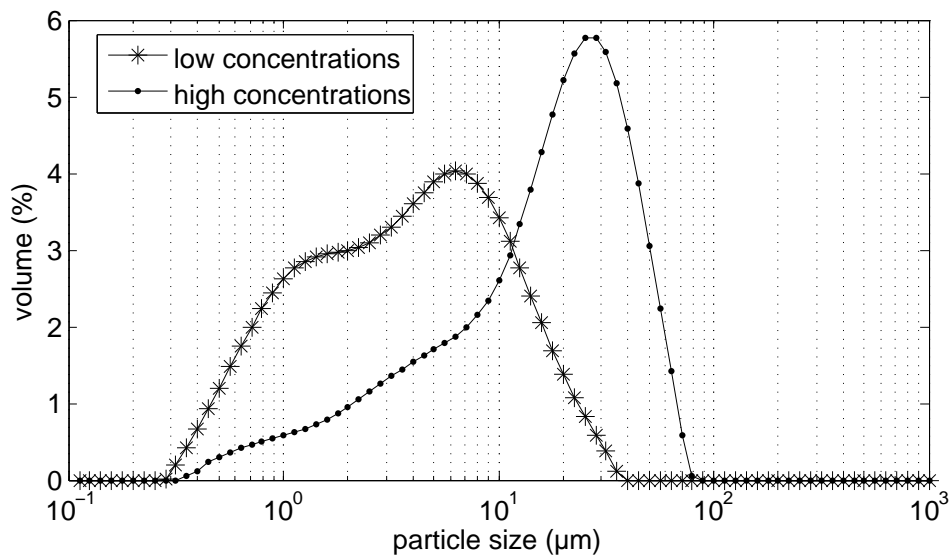


Figure 13: Particle size distributions as a function of reactants' concentrations. Parallel reactants' addition with mixing system and ultrasound are used ( $C_{\text{MgCl}_2 \cdot 6\text{H}_2\text{O}} = 0.81 \text{ mol.L}^{-1}$  and  $1.49 \text{ mol.L}^{-1}$ ,  $T=20^\circ\text{C}$ , samples taken of after 210 minutes).

The same tendency is observed at 40°C (Fig. 14).

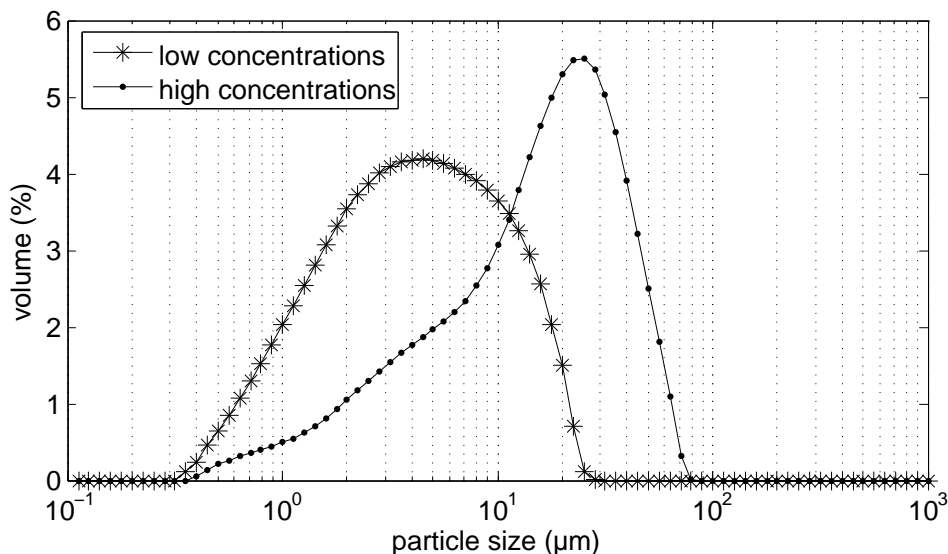


Figure 14: Particle size distributions as a function of reactants' concentrations. Parallel reactants' addition with mixing system and ultrasound are used ( $C_{\text{MgCl}_2 \cdot 6\text{H}_2\text{O}} = 0.81 \text{ mol.L}^{-1}$  and  $1.88 \text{ mol.L}^{-1}$ ,  $T=40^\circ\text{C}$ , samples taken of after 210 minutes).

233 These results are explained by the increase of supersaturation ratio at high con-  
 234 centrations. Nucleation rate also increases so more particles are synthesized. The  
 235 increase of particles number causes the increase of agglomeration phenomenon.  
 236 That's why distribution is shifted towards large particles at high concentrations.

237 Therefore, according to Zauner and Jones (2000), by increasing concentra-  
 238 tions and so supersaturation, primary particles are smaller. This result has been  
 239 confirmed by Baldyga, Makowski and Orciuch (2007). So increasing initial con-  
 240 centrations would enable to synthesize more smaller particles but to increase ag-  
 241 glomeration too.

242 When initial concentrations are higher, the specific surface area of the product  
 243 is lower:  $165 \text{ m}^2 \cdot \text{g}^{-1}$  with  $C_{\text{MgCl}_2 \cdot 6\text{H}_2\text{O}} = 1.49 \text{ mol.L}^{-1}$  as against  $350 \text{ m}^2 \cdot \text{g}^{-1}$  with  
 244  $C_{\text{MgCl}_2 \cdot 6\text{H}_2\text{O}} = 0.81 \text{ mol.L}^{-1}$  (Table 1).

### 245 3.7. Influence of synthesis temperature

246 Synthesis temperature influence on particle size is studied. Particle size distri-  
 247 butions are very similar (Fig. 15). The temperature doesn't influence the particle

248 size distributions. When temperature increases, specific surface area slightly de-  
249 creases :  $335 \text{ m}^2 \cdot \text{g}^{-1}$  at  $50^\circ\text{C}$  as against  $350 \text{ m}^2 \cdot \text{g}^{-1}$  at  $20^\circ\text{C}$  (Table 1).

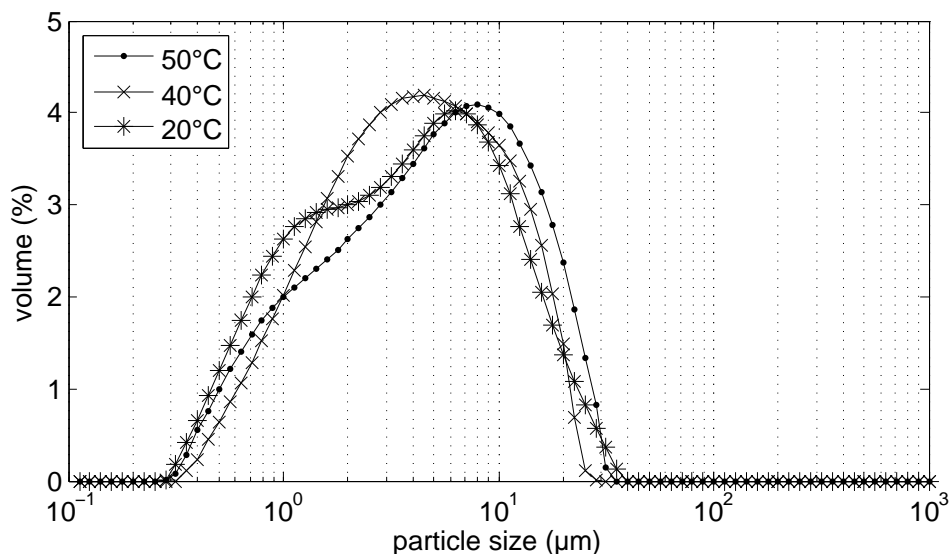


Figure 15: Particle size distributions as a function of synthesis temperature. Parallel reactants' addition with mixing system and ultrasound are used ( $C_{\text{MgCl}_2 \cdot 6\text{H}_2\text{O}} = 0.81 \text{ mol} \cdot \text{L}^{-1}$ , samples taken of after 210 minutes).

#### 250 4. Conclusions

251 Studied process parameters (reactant concentration, temperature, mixing mode)  
252 wouldn't influence crystallinity rate of synthesized product, it's amorphous in all  
253 cases. It's also very agglomerated whatever process parameters. Therefore some  
254 parameters would enable to decrease agglomerates sizes. In order to synthesize  
255 smallest agglomerates and particles, reactants' addition by the mixing system with  
256 ultrasound used during the synthesis would be the most appropriate. Median ag-  
257 glomerates size obtained with these conditions is about  $4 \mu\text{m}$ . It's bigger than  
258 the objective size but it's agglomerates size and not primary particles size. SEM  
259 analysis let think that primary particles size is about 100 nm. (Synthesis tempera-  
260 turew) Mixing mode and initial reactants' concentrations influence agglomeration  
261 phenomenon by means of the nucleation. High initial concentrations and pre-  
262 mixing would enable to synthesize more particles and so increase agglomeration  
263 phenomenon.

264 A perspective of this study is to be able to easy disaggregate product in the  
265 polymer matrix in order to obtain nanosized primary particles well-dispersed in  
266 the polymer.

### 267 **Acknowledgements**

268 The authors acknowledge the Agence Nationale de la Recherche for the finan-  
269 cial support of ANR-09-MAPR-0017 project. The authors also thank Ms S. Del  
270 Confetto, Ms C. Rolland and Ms Séverine Patry for specific surface area measure-  
271 ments, microscopy analysis and X-Ray diffraction analysis.

272 **References**

- 273 Baldyga, J., Makowski, L., Orciuch, W., 2007. Double-feed semibatch precipi-  
274 tation - effects of mixing. *Chemical Engineering Research & Design* 85, 745–  
275 752.
- 276 Ciesielczyk, F., Krysztafkiewicz, A., Bula, K., Jesionowski, T., 2010. Evaluation  
277 of synthetic magnesium silicate as a new polymer filler. *Composite Interfaces*  
278 17, 481–494.
- 279 Ciesielczyk, F., Krysztafkiewicz, A., Jesionowski, T., 2005. Influence of sur-  
280 face modification on morphology and physicochemical parameters of synthetic  
281 magnesium silicate. *Physicochemical Problems of Mineral Processing* 39, 155–  
282 164.
- 283 Ciesielczyk, F., Krysztafkiewicz, A., Jesionowski, T., 2007. Physicochemical  
284 studies on precipitated magnesium silicates. *Journal of Materials Science* 42,  
285 3831–3840.
- 286 Dodds, J., Espitalier, F., Louisnard, O., Grossier, R., David, R., Hassoun, M.,  
287 Baillon, F., Gatamel, C., Lyczko, N., 2007. The effect of ultrasound on  
288 crystallisation-precipitation processes: Some examples and a new segregation  
289 model. *Particle & Particle Systems Characterization* 24, 18–28.
- 290 Lèbre, C., 2007. Elaboration et caractérisation de talcs synthétiques pour  
291 l'amélioration des propriétés physiques des matériaux composites industriels.  
292 Ph.D. thesis. Thèse de l'Université de Toulouse III.
- 293 Martin, F., 1999. Le talc : un minéral idéal ? Habilitation à Diriger des  
294 Recherches, Université Toulouse III, Paul Sabatier.
- 295 Martin, F., Ferret, J., Lèbre, C., Petit, S., Grauby, O., Bonino, J.P., Arseguel,  
296 D., Decarreau, A., 2006. Procédé de préparation d'une composition de talc  
297 synthétique à partir d'une composition de kéroïlites. Brevet d'invention français  
298 FR2903682 - A1 - 2006.
- 299 Mersmann, A., 1999. Crystallization and precipitation. *Chemical Engineering*  
300 and Processing 38, 345–353.
- 301 Tufar, W., 2000. *Talc*. Wiley-VCH Verlag GmbH & Co. KGaA.



302 Zauner, R., Jones, A., 2000. Mixing effects on product particle characteristics  
303 from semi-batch crystal precipitation. *Chemical Engineering Research & De-*  
304 *sign* 78, 894–902.